Identification of a tumor-promoter cholesterol metabolite in human breast cancers acting through the glucocorticoid receptor

Maud Voisin[a,b,1], Philippe de Medina[c,1], Arnaud Mallinger[a,b,1], Florence Dalenc[a,b,d], Emilie Huc-Claustre[a,b], Julie Leignadier[a,b], Nizar Serhan[a,b], Régis Soules[a,b], Grégory Ségala[a,b], Aurélie Mougel[a,b], Emmanuel Noguer[a,b,c], Loubna Mhamdi[c], Elodie Bacquié[a,b], Luigi Iuliano[e], Chiara Zerbinati[e], Magali Lacroix-Triki[d], Léonor Chaltiel[d], Thomas Filleron[d], Vincent Cavaillès[f], Talal Al Saati[g], Philippe Rochaix[d], Raphaelle Duprez-Paumier[d], Camille Franchet[d], Laetitia Ligat[h], Fréderic Lopez[h], Michel Record[a,b], Marc Poirot[a,b,2], and Sandrine Silvente-Poirot[a,b,2]

[a]Team "Cholesterol Metabolism and Therapeutic Innovations," Cancer Research Center of Toulouse (CRCT), UMR 1037, Université de Toulouse, CNRS, Inserm, UPS, 31037 Toulouse, France; [b]Université Paul Sabatier, 31062 Toulouse, France; [c]Affichem, 31400 Toulouse, France; [d]Institut Claudius Regaud, Institut Universitaire du Cancer Toulouse-Oncopole, 31059 Toulouse, France; [e]Vascular Biology, Atherothrombosis & Mass Spectrometry Laboratory, Sapienza University of Rome, 04100 Latina, Italy; [f]l'Institut de Recherche en Cancérologie de Montpellier, INSERM U1194, University of Montpellier, F-34298 Montpellier, France; [g]INSERM/UPS-US006/Centre Régional d'Exploration Fonctionnelle et Ressources Expérimentales, Service d'Histopathologie, Centre Hospitalier Universitaire Purpan, 31024 Toulouse, France; and [h]Pôle Technologique, Cancer Research Center of Toulouse (CRCT), Plateau Interactions Moléculaires, INSERM-UMR1037, 31037 Toulouse, France

Edited by Christopher K. Glass, University of California, San Diego, La Jolla, CA, and approved September 15, 2017 (received for review May 13, 2017)

Breast cancer (BC) remains the primary cause of death from cancer among women worldwide. Cholesterol-5,6-epoxide (5,6-EC) metabolism is deregulated in BC but the molecular origin of this is unknown. Here, we have identified an oncometabolism downstream of 5,6-EC that promotes BC progression independently of estrogen receptor α expression. We show that cholesterol epoxide hydrolase (ChEH) metabolizes 5,6-EC into cholestane-3β,5α,6β-triol, which is transformed into the oncometabolite 6-oxo-cholestan-3β,5α-diol (OCDO) by 11β-hydroxysteroid-dehydrogenase-type-2 (11βHSD2). 11βHSD2 is known to regulate glucocorticoid metabolism by converting active cortisol into inactive cortisone. ChEH inhibition and 11βHSD2 silencing inhibited OCDO production and tumor growth. Patient BC samples showed significant increased OCDO levels and greater ChEH and 11βHSD2 protein expression compared with normal tissues. The analysis of several human BC mRNA databases indicated that 11βHSD2 and ChEH overexpression correlated with a higher risk of patient death, highlighting that the biosynthetic pathway producing OCDO is of major importance to BC pathology. OCDO stimulates BC cell growth by binding to the glucocorticoid receptor (GR), the nuclear receptor of endogenous cortisol. Interestingly, high GR expression or activation correlates with poor therapeutic response or prognosis in many solid tumors, including BC. Targeting the enzymes involved in cholesterol epoxide and glucocorticoid metabolism or GR may be novel strategies to prevent and treat BC.

breast cancer | oncometabolism | dendrogenin A | therapy | nuclear receptor

A role for cholesterol in the etiology of cancers has long been suspected, and 5,6-cholesterol epoxides (5,6-EC) were initially thought to be the causative agents. However, recent data have now shown that it is the metabolism of 5,6-EC that is deregulated in breast cancer (BC), and that this metabolism controls BC development (1–4). To develop novel precision therapeutic strategies, a deeper understanding of 5,6-EC metabolism is required. Indeed, BC remains the most frequent cause of death from cancer among women worldwide, despite the development of targeted therapies, such as Tamoxifen (Tam) for treating tumors expressing the estrogen receptor (ER), or agents that target the overexpressed growth factor receptor HER2 (human epidermal growth factor receptor). These failures are explained by the fact that many BC do not respond to these therapies or develop resistance, and there are currently no effective targeted therapies to treat tumors that express neither ER nor HER2. In addition to its role as a competitive inhibitor for ER, Tam also impacts on cholesterol metabolism by targeting cholesterol epoxide hydrolase (ChEH), an enzymatic complex formed by two cholesterogenic enzymes, DHCR7 and D8D7I (also known as EBP) (5–7). In normal tissues, ChEH catalyzes the hydrolysis of the cholesterol 5,6-epoxides α and β (5,6α-EC and 5,6β-EC) into cholestane-3β,5α,6β-triol (CT) (5, 6, 8). In normal mammalian tissues, 5,6α-EC reacts with histamine via an enzyme to produce a tumor suppressor metabolite named dendrogenin A (DDA), whose levels are significantly decreased in BC compared with normal adjacent tissues (NAT), indicating a deregulation of this pathway during BC development (3, 4). These data combined suggest a potential role of ChEH activation in BC progression that we explored in the present study. Herein, we describe how this led us to discover an oncometabolite,

Significance

Cholesterol and its transformation into cholesterol-5,6-epoxides (5,6-EC) was long suspected as contributing to breast cancer (BC) pathogenesis, before it was found that 5,6-EC metabolism controls BC development and is deregulated in breast cancers. Herein, we studied in tumor cells and human samples how 5,6-EC metabolism deregulation promotes tumor progression. We have discovered a pathway in BCs producing an oncometabolite derived from 5,6-EC, through the action of the cortisol-inactivating enzyme, and identified the glucocorticoid receptor (GR) as the target mediating its proliferative effects. Inhibition of its production or GR significantly blocked its action on BC progression. Thus, targeting this oncometabolism and GR represents a new opportunity for therapeutic intervention in BCs and potentially other cancers presenting such deregulations.

Author contributions: M.P. and S.S.-P. designed research; M.V., P.d.M., A. Mallinger, F.D., E.H.-C., J.L., N.S., R.S., G.S., A. Mougel, E.N., L.M., E.B., C.Z., M.L.-T., T.A.S., R.D.-P., C.F., L.L., M.R., M.P., and S.S.-P. performed research; M.V., P.d.M., A. Mallinger, F.D., E.H.-C., J.L., N.S., R.S., G.S., A. Mougel, E.N., L.M., E.B., L.I., C.Z., M.L.-T., L.C., T.F., V.C., T.A.S., P.R., R.D.-P., C.F., L.L., F.L., M.R., M.P., and S.S.-P. analyzed data; and M.P. and S.S.-P. wrote the paper.

Conflict of interest statement: P.d.M., E.N., and L.M. are employees of the company Affichem, of which S.S.-P. and M.P. are founders.

This article is a PNAS Direct Submission.

[1]M.V., P.d.M., and A. Mallinger contributed equally to this work.

[2]To whom correspondence may be addressed. Email: marc.poirot@inserm.fr or sandrine.poirot@inserm.fr.

This article contains supporting information online at www.pnas.org/lookup/suppl/doi:10.1073/pnas.1707965114/-/DCSupplemental.

6-oxo-cholestan-3β,5α-diol (OCDO), that drives BC progression through the glucocorticoid receptor (GR). Furthermore, we show that OCDO is derived from 5,6-ECs through the action of ChEH and the cortisol-inactivating enzyme, 11βHSD2. Inhibiting this oncometabolic pathway or GR significantly reduced BC proliferation, suggesting that targeting the actors of this pathway could represent new strategies in BC therapy and prevention.

Results

Kinetic Analysis of 5,6-EC and CT Metabolism in MCF7 Cells. We first examined the metabolism of [^{14}C]5,6α-EC, [^{14}C]5,6β-EC, and [^{14}C]CT over a 72-h period in the breast cancer cell line MCF7. Thin-layer chromatography (TLC) analyses of cell and media extracts showed that 5,6α-EC (Fig. 1 *A* and *B*) and 5,6β-EC (Fig. 1 *C* and *D*) were first converted into CT (retention factor, R*f* = 0.21) as a result of ChEH activity. However, over time, an unknown metabolite (UM), R*f* = 0.60, appeared and its level increased at the expense of the 5,6-ECs and CT. Similar experiments performed using [^{14}C]CT alone revealed that the UM was a metabolite of CT (Fig. 1 *E* and *F*).

Characterization of UM as OCDO. It has been reported that CT can be chemically oxidized into OCDO (9), so we hypothesized that the UM could be OCDO (Fig. 2*A*). In normal-phase TLC, we found that synthetic OCDO (sOCDO) and [^{14}C]OCDO had a similar retention factor (R*f* = 0.60) to that of the UM (Fig. 2 *A* and *B*, respectively). Reverse-phase HPLC (RP-HPLC) also showed a similar retention time between UM and sOCDO or [^{14}C]OCDO (R*t* = 15 min) (Fig. 2 *C* and *D*, respectively), while synthetic CT (sCT) and [^{14}C]CT had a R*t* of 10 min (Fig. 2 *C* and *D*, respectively). To confirm the identity of the UM, MCF7 cells were treated with 5,6α-EC for 72 h, then lipids were extracted and submitted to RP-HPLC. Mass spectrometric analysis of the 9- to 11-min RP-HPLC fractions (Fig. 2*D*) showed peaks of *m/z* $[M+NH_4]^+$ = 438.6 and *m/z* $[M+N_2H_7]^+$ = 455.6, corresponding to the mass of CT and consistent with the transformation of 5,6α-EC into CT by ChEH (Fig. 2*E*). Analysis of the 15- to 17-min RP-HPLC fractions (Fig. 2*D*) showed peaks of *m/z* $[M_{UM}+NH_4]^+$ = 436.6 and *m/z* $[M_{UM}+N_2H_7]^+$ = 453.6 (Fig. 2*F*), corresponding to the mass of sOCDO. This confirmed that the UM was OCDO (Fig. 2*G*).

ChEH Inhibition Abrogates OCDO Formation in BC Cells. We next measured the impact of DDA and other ChEH inhibitors (3, 5) on OCDO formation by incubating human MCF7 or MDA-MB-231 tumor cells (expressing or not the ERα, respectively) with [^{14}C]5,6α-EC and the indicated ChEH inhibitors. As shown in Fig. 3 *A* and *B*, in both cell lines DDA and the ChEH inhibitors tested inhibited OCDO production, including ChEH inhibitors known to have antitumor activity and to inhibit ERα, such as Tam or raloxifene, or to act independently of the ERα, such as DDA, tesmilifene, or PBPE (1-[2-[4-(phenylmethyl)phenoxy] ethyl]-pyrrolidine) (3, 5, 10). These data indicate that all of these ChEH inhibitors target the OCDO pathway independently of ERα expression.

OCDO Stimulates BC Cell Proliferation in Vitro and in Vivo. Treatment with OCDO or 17β-estradiol (E2) significantly increased the growth rate of ER$^+$ cell lines (Fig. 3 *C* and *D*). OCDO also increased the proliferation of the ER$^-$ cells lines MDA-MB231 and MDA-MB468 (Fig. 3 *E* and *F*). OCDO significantly promoted the growth of both ER$^+$ and ER$^-$ tumors grafted onto mice (Fig. 3 *G* and *K*). Histological analysis of tumors revealed

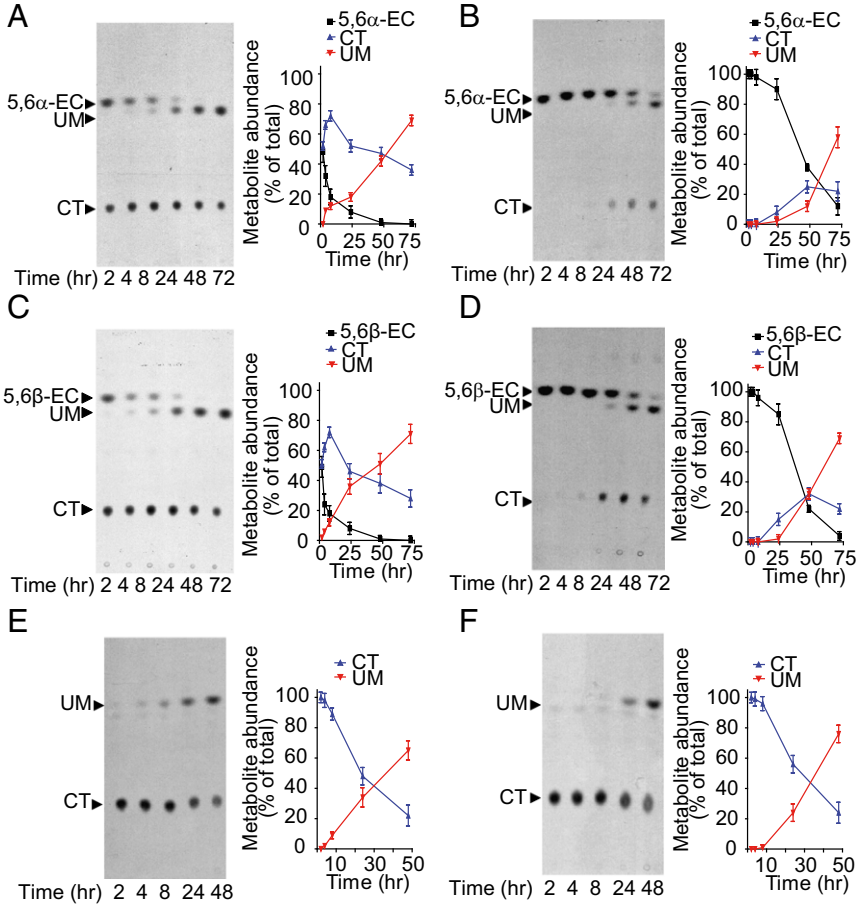

Fig. 1. UM is a metabolite of CT in tumor cells. (*A–F*, *Left*) Representative TLC autoradiograms (n = 5) showing time-dependent production of UM in MCF7 cells treated with (*A* and *B*) 600 nM [^{14}C]5,6α-EC, (*C* and *D*) 600 nM [^{14}C]5,6β-EC, and (*E* and *F*) 1 μM [^{14}C]-CT. (*Right*) Quantitative analyses of the metabolites extracted from cells (*A*, *C*, and *E*) and media (*B*, *D*, and *F*). The regions corresponding to the radioactive metabolites of interest (arrows) were recovered and counted using a β-counter. Results are the mean (±SEM) of five independent experiments.

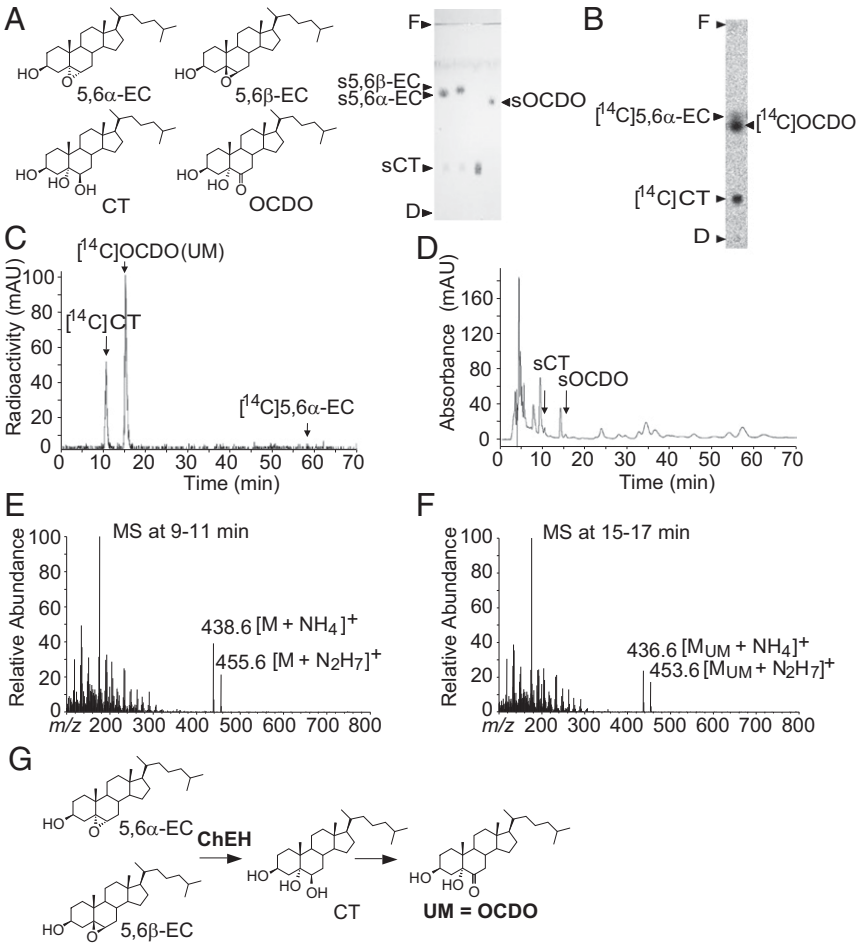

Fig. 2. Structural characterization of UM. (*A*, *Left*) Chemical structure of the metabolites of interest. (*Right*) Representative migration performed by silica gel TLC ($n = 5$) of the synthetic (s) metabolites of interest, indicated by arrows. (*B*) MCF7 cells were incubated for 72 h with [^{14}C]5,6α-EC and analyzed as described for Fig. 1 ($n = 5$). Analysis of cell extracts by (*B*) polar silica gel TLC or (*C*) hydrophobic RP-HPLC. (*D*) RP-HPLC profile of the metabolites extracted from MCF-7 cells that had been treated for 72 h with 5,6α-EC. Arrows indicate peaks corresponding to the authentic standards: sCT and sOCDO. (*E*) CI-MS spectra of the RP-HPLC peak eluted between 9 and 11 min in *D*. (*F*) CI-MS spectra of the RP-HPLC peak eluted between 15 and 17 min in *D*. (*G*) Scheme describing the formation of OCDO.

that the proliferative marker K_i67 was increased following OCDO treatment (Fig. 3*L*).

Inhibition of OCDO Production Contributes to the Antitumor Activities of DDA in Mice. We then determined whether the antiproliferative effects of DDA involved the inhibition of OCDO production. As shown in Fig. 3*M*, DDA significantly inhibited the growth of tumors compared with vehicle-treated mice. However, when OCDO was added back by treating engrafted animals with DDA plus OCDO, the growth inhibitory action of DDA was reversed, indicating that the inhibition of OCDO production contributed to the antitumor activity of this compound.

Identification of the Enzymes That Regulate the Production of OCDO from CT. Since OCDO is produced from CT, we hypothesized the existence of an enzyme distinct from ChEH that would realize this reaction. We considered that a hydroxysteroid dehydrogenase (HSD) could catalyze the dehydrogenation of the alcohol function in position 6 of CT into a ketone in OCDO. A local symmetry axis on the steroid backbone makes positions 11β and 7α equivalent (11), which suggested to us that an 11βHSD enzyme was a good candidate for catalyzing this reaction. 11βHSD exist as two enzymes, 11βHSD type 2 (11HSD2), which catalyzes the dehydrogenation of cortisol into the inactive cortisone, and 11βHSD type 1 (11HSD1), which performs the reverse reaction (12) (Fig. 4*A*). In accordance with this hypothesis, 11HSD2 mRNA and protein expression was measured in a panel of human BC cell lines expressing or not ERα, while 11HSD1 expression was not detectable and all of the cell lines tested produced OCDO (Fig. S1*A* and Table S1).

To confirm a role for 11HSD2 in the production of OCDO from CT, we transfected HEK293 cells, a cell model that has previously been used to study 11HSD1 and 11HSD2 (13), with a plasmid encoding either 11HSD2 or the empty vector (mock) (Fig. S1*B*). When incubated with [^{3}H]cortisol ([^{3}H]-CRT) (Fig. 4*B*) or [^{14}C]CT (Fig. 4*C*), 11HSD2-transfected cells produced significantly higher levels of cortisone or OCDO, respectively, than mock-transfected cells, indicating that 11HSD2 is able to produce OCDO in addition to cortisone. To study the involvement of 11HSD1 in the reverse transformation of OCDO into CT (Fig. 4*A*), HEK293T cells were transfected with a plasmid encoding 11HSD1 (HSD1) or the empty vector (mock), and with or without a plasmid encoding H6PD, the enzyme that produces the NADPH cofactor that is necessary for the reductase activity of 11HSD1 (14) (Fig. S1*C*). When cells were incubated with [^{3}H]cortisone (Fig. 4*D*) or [^{14}C]OCDO (Fig. 4*E*), 11HSD1-transfected cells produced significantly more cortisol or CT, respectively, than mock- or H6PD-transfected cells. This production was further increased by two- and fourfold, respectively, by cotransfecting 11HSD1 with H6PD. Thus, 11HSD1 produces significant levels of CT in addition to cortisol.

Ectopic 11HSD1 Expression in MCF-7 Cells Produces CT and Decreases Cell Proliferation, and OCDO Treatment Reverses This Effect. The expression of 11HSD1 in MCF7 cells (Fig. S1*D*) significantly stimulated the conversion of OCDO to CT compared with controls (Fig. 4*F*). In addition, 11HSD1 expression in MCF7 cells also significantly decreased cell proliferation, an effect that was reversed by OCDO treatment (Fig. 4*G*). This indicates that 11HSD1 inhibits tumor cell proliferation through the transformation of OCDO into CT.

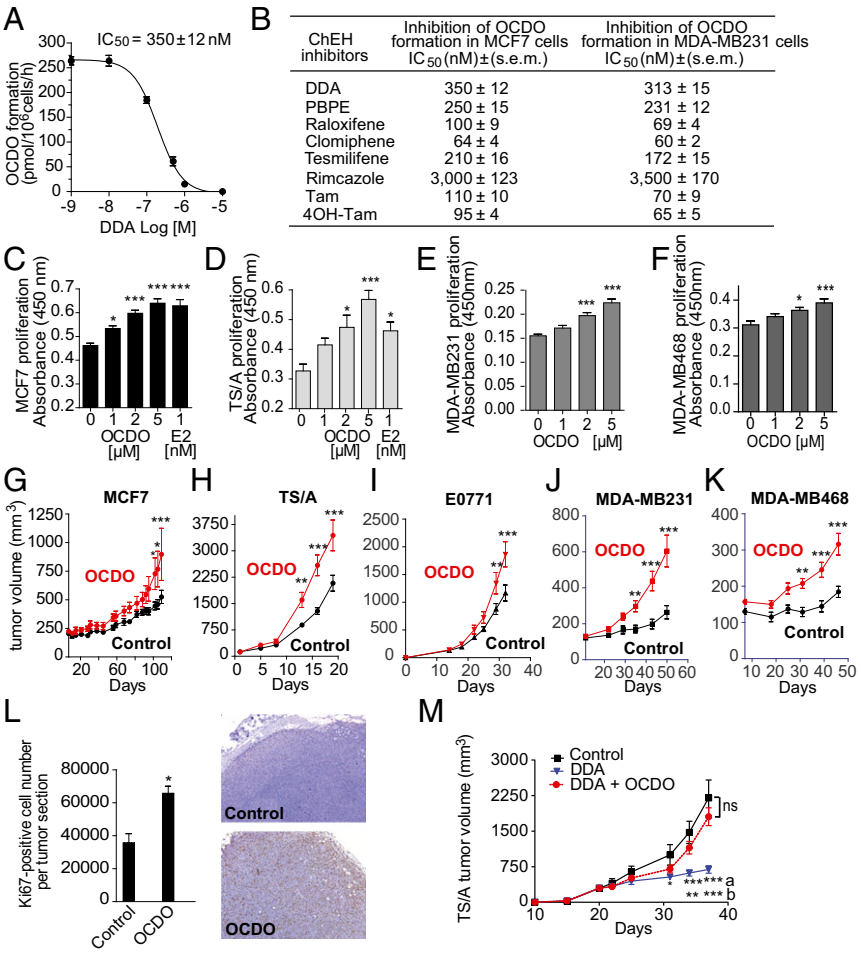

Fig. 3. OCDO is a tumor promoter and its inhibition contributes to the antitumor effects of DDA. (*A*) Representative inhibition curve showing the inhibition of OCDO formation by increasing concentrations of DDA in human MCF7 cells treated with 600 nM [^{14}C]5,6α-EC for 72 h. OCDO formation was quantified after TLC analysis as described for Fig. 1 and IC_{50} value was calculated from the concentration-inhibition curve. (*B*) Analysis of the inhibition of OCDO formation in MCF7 and MDA-MB231 cells treated as in *A* with increasing concentrations of the indicated ChEH inhibitors. OCDO formation and IC_{50} values were measured as in *A*. (*C*–*F*) Tumor cell proliferation using a colorimetric BrDU immunoassay, $n = 8$. $^{*}P < 0.05$, $^{***}P < 0.001$, one-way ANOVA, Tukey's posttest. (*A*–*F*) Data are the mean (±SEM) of five separate experiments. (*G*–*K*) Mice (10 per group) implanted with the indicated cell lines were treated with the solvent vehicle or OCDO and monitored for tumor growth over time. (*L*, *Left*) Mean (±SEM) of Ki67-positive cells quantified from IHC staining of MCF7 tumor sections from *G*, $n = 8$. $^{*}P < 0.05$, Student's *t* test, two-tailed; $^{***}P < 0.001$. (*Right*) Representative K_i67 staining of TS/A tumor sections from *H*. (*M*) Mice (10 per group) implanted with TS/A cells were treated every day, starting at day 1, with either the solvent vehicle, DDA (0.37 μg/kg), or DDA (0.37 μg/kg) + OCDO (50 μg/kg). (*G*–*K* and *M*) Data are representative of three independent experiments. Mean tumor volumes (±SEM) are shown, two-way ANOVA, Bonferroni posttest, $^{*}P < 0.05$, $^{**}P < 0.01$, $^{***}P < 0.001$. In *M*, letters indicate the comparison between: a: DDA vs. control; b: DDA vs. DDA + OCDO. ns: not significant at each time.

11HSD2 Controls Cell Proliferation and Tumor Growth Through OCDO Production. To confirm that 11HSD2 produces OCDO and stimulates tumor cell proliferation, we knocked down 11HSD2 expression in MCF7 cells using shRNA. Two stable clones (shHSD2A and shHSD2B) were selected in which the expression of 11HSD2 was significantly decreased at both the protein and mRNA levels compared with shRNA control clones (shCA and shCB) (Fig. S1*E*). A significant decrease in cortisone (Fig. 4*H*) and OCDO (Fig. 4*I*) production was measured in shHSD2A cells compared with shCA cells, and their doubling time increased by 150% (Fig. 4*J*). In addition, OCDO significantly increased ShCA cell proliferation and rescued the decreased proliferation of shHSD2A cells (Fig. 4*K*), while no such effect was observed with cortisone (Fig. 4*L*). Moreover, OCDO also significantly increased ShCA clonogenecity and rescued the decreased clonogenicity of 11HSD2A cells (Fig. 4*M*). Together, these results indicate that 11HSD2 controls cell proliferation and clonogenicity through OCDO production. We then tested the impact of 11HSD2 knockdown in vivo by implanting shHSD2A cells into mice. As shown in Fig. 4*N*, the growth of shHSD2A tumors was significantly reduced (by 50%) compared with shCA tumors. Importantly, OCDO significantly stimulated the growth of ShCA tumor and rescued the decrease growth of shHSD2A tumors, indicating that 11HSD2 controls tumor growth through OCDO production. Similar results, both in vitro and in vivo, were obtained with the other shHSD2B and shCB clones (Fig. S1 *F*–*K*). To confirm the involvement of 11HSD2 in cell proliferation, MCF7 cells were stably transfected with a plasmid expressing 11HSD2 or the control plasmid. Two clones stably overexpressing 11HSD2 and two control clones (mock) were selected (Fig. S1*L*). The clones overexpressing 11HSD2 showed a greater capacity to produce OCDO when incubated with [^{14}C]CT (Fig. S1*L*) and proliferated significantly faster in vitro, indicating an effect on tumor cells (Fig. 4*O*), and in vivo when implanted into mice, compared with control clones (Fig. 4*P* and Fig. S1*M*).

Enzymes Involved in the Production of OCDO Are Overexpressed in Human BC Compared with Matched Normal Adjacent Breast Tissue. We then compared the expression of enzymes regulating OCDO production (namely 11HSD2, DHCR7, D8D71/EBP, 11HSD1, H6PD) in 50 patient BC samples with matched NAT, by immunohistochemistry (IHC). Patient characteristics are summarized in Table S2. As shown in Fig. 5*A* and Fig. S2*A*, 11HSD2 expression was significantly higher in BC than in matched NAT. In addition, a positive correlation was found between the expression of 11HSD2 in BC and grade III tumors (Table S3). In contrast, 11HSD1 and H6PD were weakly present in both BC and NAT samples, with no significant difference between their expression levels in the two tissues (Fig. 5*A* and Fig. S2*A*). D8D7I (EBP) and DHCR7, which together make up the ChEH, had a significantly higher expression in tumors compared with NAT (Fig. 5*A* and Fig. S2*A*) and their expression positively correlated with each other in tumors ($r = 0.43$; $P = 0.004$). The expression of the two ChEH subunits was also highly significantly correlated at the mRNA level ($r = 0.37$; $P < 0.0001$) (Fig. S2*B*). These data are in agreement with the fact that the two enzymes work together for an optimal ChEH activity (5). A positive correlation was also found between the expression of DHCR7 and grade III tumors. In addition, ER^{-}/PR^{-} patients had a significant increased proportion of tumors expressing high levels of DHCR7 and D8D7I. In contrast, a high level of 11HSD2 appeared independent of hormone receptor status (Table S3). At the mRNA

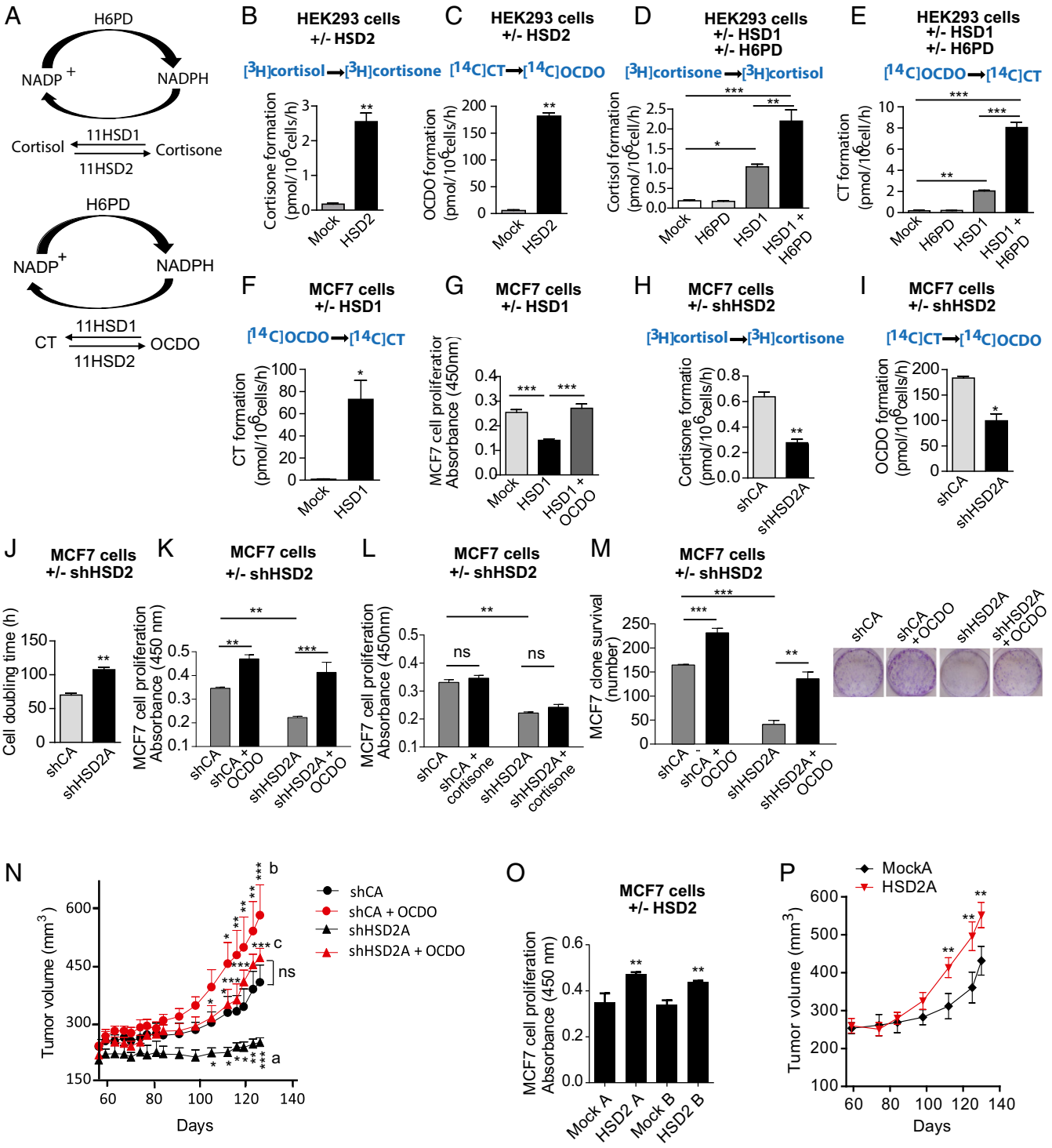

Fig. 4. 11βHSD2 and 11βHSD1 interconvert OCDO and CT. (*A*, *Upper*) 11HSD2 catalyzes the dehydrogenation of cortisol into cortisone. 11HSD1 realizes the reverse reaction. H6PD is the enzyme that produces the cofactor NADPH necessary for the reductase activity of 11HSD1. (*A*, *Lower*) 11HSD2 produces OCDO from CT and 11HSD1 produces CT from OCDO. (*B–M* and *O*) HEK293T (HEK) or MCF7 cells were transfected with plasmids encoding the indicated enzyme or the empty vector (mock) or shRNA. (*B–F*) The production of the indicated metabolites in transfected HEK (*B–E*) or MCF7 cells (*F*) was analyzed as in Fig. 1, $n = 5$. (*G*) The proliferation of transfected MCF7 cells was analyzed as in Fig. 3 *C–F*, $n = 8$. (*H–M*) shCA- and shHSD2A-MCF7 cells were assayed for: (*H*) cortisone or (*I*) OCDO production, as measured in Fig. 1, $n = 5$; (*J–L*) cell proliferation by (*J*) counting cell numbers, $n = 5$, or (*K–L*) as in *G*, $n = 8$; or (*M*) cell clonogenicity ($n = 3$), with or without 5 μM OCDO or cortisone. (*N*) shCA or shHSD2A-MCF7 tumors engrafted into mice (10 per group) were treated with solvent vehicle (control) or OCDO (16 μg/kg, 5 d/wk). Data are representative of three independent experiments. (*O*) Control (mock) or HSD2 overexpressing MCF7 cell proliferation was analyzed as in *G*. (*P*) The growth of control (mock) or 11HSD2 overexpressing MCF7 tumors engrafted into mice (10 mice per group) were compared over time. Data are representative of three independent experiments. (*B–M* and *O*) Data are the mean (±SEM) of five separate experiments and were analyzed (*B*, *C*, *F*, and *H–J*) by a Student's *t* test, two-tailed, or (*D*, *E*, *G*, and *K–O*) by one-way ANOVA, Tukey's posttest. $^*P < 0.05$, $^{**}P < 0.01$, $^{***}P < 0.001$. (*N* and *P*) Mean tumor volumes (±SEM) are shown, and data were analyzed by two-way ANOVA, Bonferroni posttest. $^*P < 0.05$, $^{**}P < 0.01$, $^{***}P < 0.001$. In *N*, letters indicate the comparison between: a: shCA vs. shHSD2A; b: shCA vs. shCA + OCDO; c: shHSD2A vs. shHSD2A + OCDO.

level, both ChEH subunits were also expressed in the more aggressive molecular subtypes (i.e., basal, luminal B, and mApo) (15) (Fig. S2 *C* and *D* and Table S4). Taken together, these results indicate that the enzymes involved in the production of OCDO are more highly expressed in BC relative to NAT, while those involved in its conversion are weakly expressed.

Levels of OCDO and Its Precursors Are Higher in Patient BC Samples Compared with Normal Tissues. We then quantified the levels of OCDO and its precursors in 16 paired patient BC and NAT by gas chromatography coupled to mass spectrometry (GC/MS). The levels of OCDO (Fig. 5*B*) and its precursors CT, 5,6α-EC, and 5,6β-EC (Fig. 5*C*) were significantly higher in patient tumors compared with NAT ($P = 0.0245$, 0.0162, 0.0121, and 0.0077, respectively; Wilcoxon test for paired samples, two-tailed), indicating that the increased expression of 11HSD2 and the ChEH subunits in BC favors the production of OCDO. To determine whether OCDO concentration used to treat mice was relevant to the pathological conditions, we measured OCDO levels in TS/A tumors treated or not with 50 μg/kg OCDO for 19 d (Fig. 3*H*) by GC/MS. The mean levels of OCDO measured in control tumors were of 197 ± 44 ng/g tissue (~0.5 μM) and significantly increased to 458 ± 91 ng/g tissue in OCDO-treated tumors (~1 μM) (Fig. 5*D*). These levels are within the pathological levels found in human tumors (mean: 357 ± 183 ng/g tissue, ~0.85 μM) (Fig. 5*B*). We also measured the physiological levels of OCDO in six normal breast samples (Fig. 5*E*). The median level of OCDO measured in these normal samples was 10.6 ng/g tissue (range: 3.4–21.7; ~25 nM) and was not significantly different from the median level of OCDO measured in NAT (Fig. 5*B*), 14.1 ng/g tissue (range: 7.5–1,350; $P = 0.0768$, Mann–Whitney test; ~33 nM).

Expression of the Enzymes Producing OCDO in BC Correlates with Patient Survival. The BreastMark algorithm was used to perform Kaplan–Meier analysis on several datasets (16). Low levels of 11HSD1 (*HSD11B1*) mRNA and high levels of 11HSD2 (*HSD11B2*) mRNA were significantly associated with a poor prognosis (decreased overall survival rate) (Fig. 6 *A* and *B*). As shown in Fig. 6 *C* and *D* and Fig. S2*E*, high levels of EBP (D8D7I) and DHCR7 mRNA were also significantly associated with a lower survival rate of patients. Interestingly, the discrimination between the overall survival rates of patients using DHCR7 or EBP (D8D7I) mRNA levels was also found using other online databases, such as Breast Cancer Gene-Expression Miner and Kaplan–Meier Plotter (Fig. S2*F*). When the expression levels of 11HSD2, DHCR7, and EBP (D8D7I) were taken into account, the risk of death was the highest [hazard ratio (HR) = 1.849] (Fig. 6*E*). Altogether, these data demonstrate that a high expression level of the enzymes involved in the pathway producing OCDO correlates with lower patient overall survival rates.

OCDO Binds to the GR, Liver X-Receptors, but Not ERα. Since OCDO and cortisol production are regulated by the same enzymes, we tested whether OCDO can bind to the GR, the cortisol receptor. In addition, the oxysterol 27-hydroxycholesterol has been shown to act through the ERα and the liver-X-receptors (LXRs) (17, 18); therefore, we investigated whether OCDO interacts with these receptors. Surface plasmon resonance (SPR) assays indicated that OCDO binds to the ligand binding domain (LBD) of the GR, as observed with the positive control cortisol (Fig. 6*F*), and to the LBD of the LXR subtypes α and β (LXRα and LXRβ), as observed with the LXR ligand, 22(R)hydroxycholesterol [22(R)HC] (Fig. S3 *A*–*D*). In contrast, we did not detect any interaction

A

Enzyme	Tumor n	Tumor Global expression SI score [1-3] (%)	Tumor High expression SI score [2-3] (%)	Normal adjacent tissue n	Normal adjacent tissue Global expression SI score [1-3] (%)	Normal adjacent tissue High expression SI score [2-3] (%)	p-value
11HSD2	45	97.8	64.4	42	19	2.4	<0.0001
DHCR7	46	87	45.7	42	81	11.9	0.0001
D8D7I (EBP)	46	100	45.7	42	73.8	19	0.0045
11HSD1	45	24.4	4.4	41	39	2.4	ns
H6PD	42	38.1	16.7	39	46.2	12.8	ns

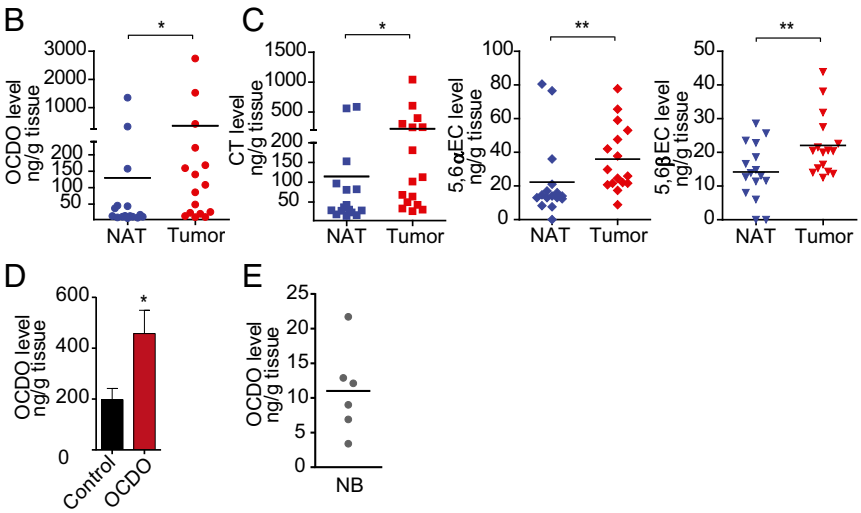

Fig. 5. Expression levels of the enzymes regulating OCDO production and dosage of their metabolites in patient samples. (*A*) IHC analyses using specific antibodies against the enzymes of interest (Table S5). SI, Staining intensity score. Enzyme expression in BC and NAT was analyzed using the McNemar test for paired samples. (*B* and *C*) The indicated endogenous metabolites levels were quantified by GC/MS in matched patient tumors and NAT ($n = 16$). $^*P < 0.05$, $^{**}P < 0.01$, Wilcoxon test for paired samples, two-tailed. (*D*) OCDO level was quantified by GC/MS in TS/A tumors implanted into mice treated with 50 μg/kg OCDO for 19 d or treated with solvent vehicle (control) ($n = 10$ mice per group). Mean OCDO levels (±SEM), $n = 10$, are shown, $^*P < 0.05$, Mann–Whitney test, two-tailed. Data are representative of three independent experiments. (*E*) Endogenous OCDO level was quantified by GC/MS in normal breast (NB) samples ($n = 6$). (*B*, *C*, and *E*) Each point represents the mean level of the metabolite of interest analyzed twice.

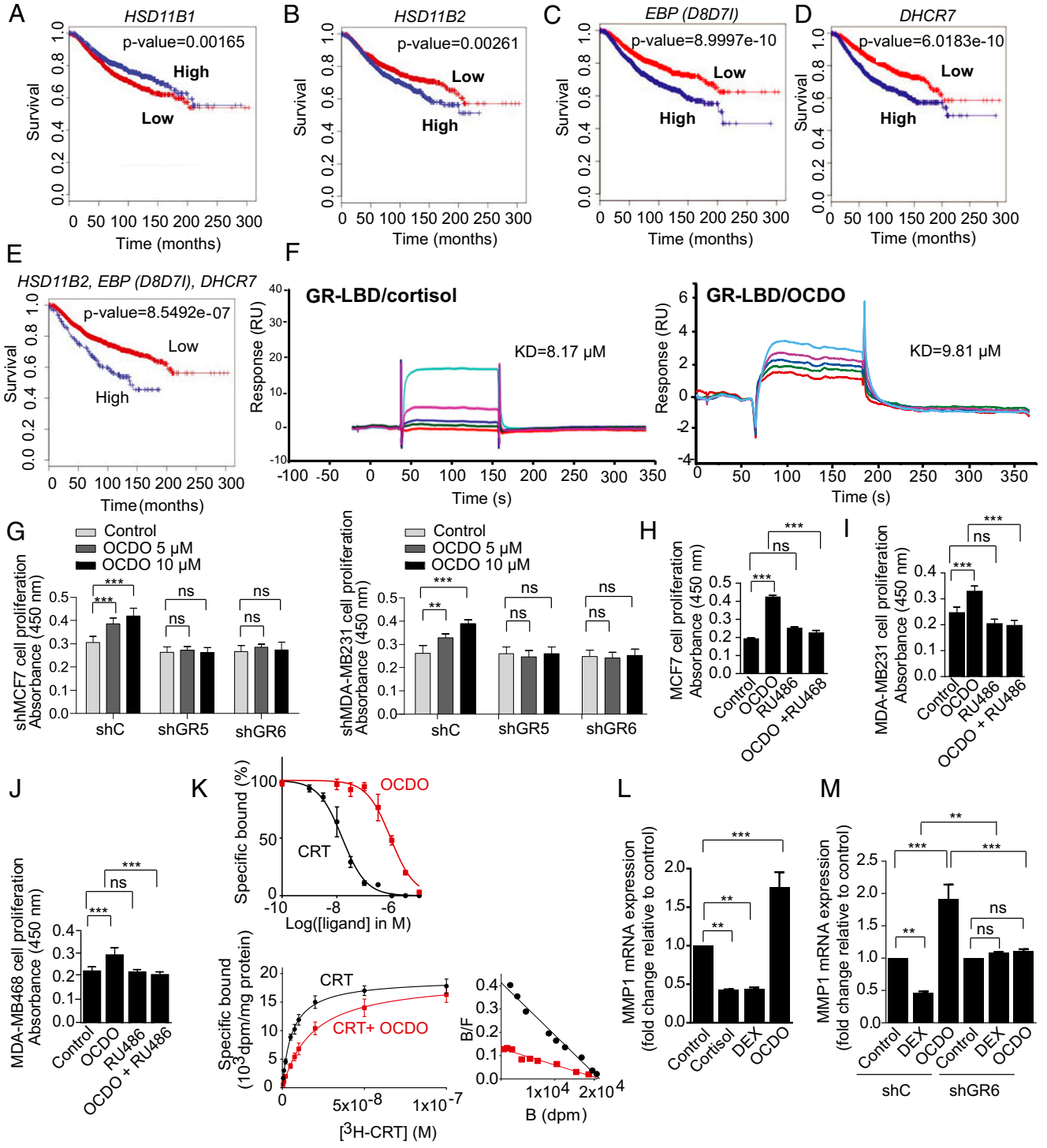

Fig. 6. Expression of the enzymes regulating OCDO production and patient survival, and evidence that OCDO binds and stimulates cell proliferation through the GR and regulates GR transcriptional activity. (*A–D*) Kaplan–Meier representation of patient overall survival according to the indicated enzyme expression (median cut-off) using the BreastMark mining tool on 21 individual datasets (4,738 samples). Survival curves are based on Kaplan–Meier estimates and log-rank *P* values were calculated for differences in survival. Cox regression analysis was used to calculate HRs. (*E*) Kaplan–Meier representation of patient overall survival taking into account the expression of the HSD11B2, EBP (D8D7I), and DHCR7 genes using the BreastMark mining tool. (*F*) Representative SPR sensorgrams from three experiments showing the binding of a series of concentrations of cortisol or OCDO (µM) to the GR-LBD captured on a Biacore sensor chip: 6.25 (red); 12.5 (green); 25 (dark blue); 50 (pink); 100 (light blue). (*G–J*) Proliferation of the indicated tumor cells was analyzed as in Fig. 3C, $n = 8$. (*H–J*) The indicated tumor cells was treated with either the solvent vehicle (control), 5 µM OCDO, 1 µM RU486, or 5 µM OCDO plus 1 µM RU486. Data are the means (±SEM) of five separate experiments, $n = 8$, $^{**}P < 0.01$, $^{***}P < 0.001$, one-way ANOVA, Tukey's posttest. (*K*, *Upper*) Cell cytosols were incubated with 10 nM [^{3}H]-CRT and increasing concentrations of unlabeled CRT or OCDO for competition binding assays. (*K*, *Lower*) Saturation and scatchard plots analyses were performed with cell cytosols incubated with increasing concentration of [^{3}H]-CRT in the absence or in the presence of 1 µM unlabeled CRT (nonspecific binding) or 1 µM OCDO for competitivity studies. Data are the mean (±SEM) of triplicate and are representative of three experiments. (*L* and *M*) qRT-PCR analysis of MMP1 gene expression in MDA-MB231 (*L*) or shC and shGR MDA-MB231 (*M*) cells treated either with the solvent vehicle (control), 0.5 µM cortisol, 0.1 µM DEX or 5 µM OCDO. (*L* and *M*) Data are the means ± SEM of three experiments performed in triplicate, $^{**}P < 0.01$, $^{***}P < 0.001$, one-way ANOVA, Tukey's posttest. ns, not significant.

between OCDO and the LBD of ERα, whereas 17β-estradiol binds to the ERα (Fig. S3 *E–F*). These data indicate that OCDO binds to the GR and the LXRs but not ERα.

OCDO Mediates Tumor Cell Proliferation Through the GR and Regulates GR Transcriptional Activity. To determine the involvement of GR and LXRs in OCDO-induced tumor cell proliferation, we knocked down the expression of GR or LXRβ, the only isoform present in MCF7 and MDA-MB231 cells (19), using shRNA. Two stable clones with significantly decreased GR and LXRβ expression (shGR or shLXR) compared with control clones (shC) were selected (Fig. S3 *G* and *H*). GR knockdown in MCF7 and MDA-MB231 cells abolished the cell proliferation induced by OCDO (Fig. 6*G*) and RU486 (Mifepristone), a GR antagonist, completely abolished OCDO-induced cell proliferation in MCF7, MDA-MB231, and MDA-MB468 tumor cell lines (Fig. 6 *H–J*). In contrast, the knockdown of LXRβ did not affect OCDO-mediated cell proliferation in either tumor cell lines (Fig. S3*I*). These data indicate that the proliferative effect of OCDO is dependent of the GR, but not of the LXRβ. We then tested whether the synthetic agonist dexamethasone (DEX) could inhibit tumor cell proliferation induced by OCDO. DEX inhibited basal and OCDO-induced MCF7 and MDA-MB231 cell proliferation at 1 μM concentration but had no effect at lower concentrations (Fig. S3*J*). To determine whether OCDO is or not a competitive inhibitor of cortisol on the GR, we performed competition binding experiments on lysates of GR-transfected cells using [^{3}H]-CRT (Fig. 6*K*). OCDO fully inhibited [^{3}H]-CRT binding to the GR in a concentration-dependent manner with an IC_{50} of 0.91 ± 0.12 μM and a K_i of 0.3 ± 0.07 μM (Fig. 6*K*, *Upper*). Saturation analyses showed that cortisol bound to the GR with a K_d of 5.9 ± 0.5 nM (Bmax of 0.92 ± 0.18 pmol/mg proteins). OCDO, at 1 μM, decreased the affinity of cortisol (K_d = 17.8 ± 3.1 nM) without changing the Bmax, indicating that OCDO is a competitive inhibitor of cortisol on the GR (Fig. 6*K*, *Lower*).

After binding to active glucocorticoids, GR translocates from the cytoplasm to the nucleus, where it positively or negatively regulates the expression of glucocorticoid-responsive genes via different mechanisms, including transactivation via the binding of liganded-GR to glucocorticoid-response elements (GREs) or repression via the binding of a negative GRE (nGRE) or transrepression via its interaction with other transcription factors, such as activator protein-1 or NFκB (20, 21). To determine whether, OCDO regulates GR transcriptional activity, OCDO was first tested for its ability to translocate GR into the nucleus in comparison with glucocorticoids (cortisol). As observed in Fig. S4*A*, in vehicle-treated MDA-MB231 cells, GR is mostly localized in the cytoplasm in an inactive form. Addition of either cortisol or OCDO to MDA-MB231 cells caused a significant eightfold and sixfold increase in GR nuclear localization. We next determined whether OCDO regulates the transcriptional activity of GR in MDA-MB231 cells by evaluating the transcription of canonical endogenous genes regulated by GR, such as SGK1 and MKP1, which are activated (22, 23), or MMP1 (collagenase), which is repressed by cortisol or dexamethasone (24). As shown in Fig. S4*B*, cortisol significantly increased SGK1 and MKP1 gene expression compared with vehicle-treated cells while OCDO had no significant effect on the transcription of these genes. When cells were treated with OCDO plus cortisol, SGK1 and MKP1 expression was significantly decreased compared with cortisol alone. In contrast, cortisol and DEX significantly inhibited the transcription of the MMP1 gene, while OCDO significantly stimulated its transcription (Fig. 6*L*). The induction of MMP1 gene transcription by OCDO through the GR was confirmed in control or GR-knockdown MDA-MB231 cells (ShC and shGR). The up-regulation of MMP1 mRNA by OCDO measured in shC cells was abolished in shGR cells and the inhibition of MMP1 mRNA by DEX in shC cells was reversed to basal in shGR cells (Fig. 6*M*). Taken together, these data indicate that OCDO regulates positively or negatively GR transcriptional activity by binding to the GR and inducing its nuclear localization. OCDO was next evaluated for its capacity to regulate the transcriptional activity of other nuclear receptors known to be regulated by oxidation products of cholesterol, such as the retinoid orphan-related receptors α and γ (RORα and RORγ) (25, 26) and the farnesoid X receptor (FXR) (27). OCDO did not regulate positively or negatively the transcriptional activity of these receptors as observed with their ligands (Fig. S4*C*).

We then analyzed the effects of OCDO on cell cycle progression in shC and ShGR MDA-MB231 cells. As shown in Fig. S4*D*, OCDO induced cell cycle progression by decreasing the percent of the G0/G1 phase and increasing the S and G2/M phases in shC cells. These effects were not observed in shGR cells treated with OCDO. These data confirm the mechanism of GR-dependent promotion of tumor cell proliferation by OCDO.

Discussion

Our study reveals that 5,6-EC can be metabolized into an oncometabolite, identified by MS as the oxysterol OCDO, and that it is found at significant greater levels in BC compared with normal tissues. We have shown that several enzymes are involved in the biosynthetic pathway that leads to OCDO production: ChEH, which is formed by D8D7I and DHCR7, and which mediates the transformation of 5,6-EC into CT (5, 6); and 11HSD2, which is involved in the final step in the transformation of CT into OCDO. We found that 11HSD2 controls BC cell proliferation both in vitro and in vivo through OCDO production. 11HSD2 is known to regulate glucocorticoid metabolism by converting active cortisol into inactive cortisone (12). In this study, we have shown that OCDO binds to the GR and LXRs but not to ERα. Moreover, OCDO stimulates the growth of BC cells and cell cycle progression irrespective of their ERα expression status by acting through the GR. Thus, the properties and mechanism of action of OCDO are distinct from another oxysterol, 27-hydroxycholesterol (27-HC), which increases the growth of ERα$^+$ BC cells by interacting with ERα (17, 18). 27-HC also interacts with the LXRβ in BC cells to mediate tumor cell invasion, but not proliferation as observed with OCDO (17, 18). Therefore, the effect of OCDO on tumor cell invasion and the involvement of LXRβ in this event should be explored in the future. Competitive binding experiments indicate that OCDO inhibits cortisol binding to the GR with a K_i of 0.30 ± 0.07 μM and that it is a competitive inhibitor of cortisol. The concentration of OCDO in mouse xenografts or in patient tumors was estimated to be around 0.5 and 0.85 μM, respectively. These concentrations are close to the K_i value of OCDO for the GR.

OCDO, like the agonist cortisol, causes the translocation of the GR from the cytoplasm to the nucleus to regulate positively or negatively GR target gene transcription (20, 21). OCDO does not stimulate the transcription of SGK1 or MKP1/DUSP1 genes, as observed with cortisol, while OCDO inhibits the induction of the transcription of these genes by cortisol. In addition, OCDO increases MMP1 gene expression by acting through the GR, while cortisol or DEX represses MMP1 gene transcription. We have found that DEX inhibits the basal and OCDO-induced MCF7 and MDA-MB231 cell proliferation, but only at 1 μM, consistent with data from the literature showing that DEX inhibits tumor cell proliferation at high concentrations (28). Combined, these data suggest that OCDO and glucocorticoids, while acting through the GR, have distinct mechanisms of action on GR transcription and cell proliferation. In a nonexhaustive way, this could be explained by the recruitment of different cofactors, which will determine GR activation or repression activity, or by posttranslational modifications of the GR, such as phosphorylation, since ligand-selective GR phosphorylation has been shown to correlate with levels of GR transcriptional activity (29). Interestingly, a recent study comparing the pharmacodynamics of different GR ligands in activating gene expression showed that ligands elicit differential activation of distinct genes, where ligand-intrinsic efficacy and GR density were essential determinants (30). Thus, additional work will be required to

elucidate the molecular mechanisms underlying the proliferative effect of OCDO mediated by the GR and the profile of the genes involved. The effects of OCDO are opposite to those of DDA, which inhibits BC progression (3, 31). Both compounds arise from 5,6-ECs; however, only 5,6α-EC generates DDA (3), while both 5,6α-EC and 5,6β-EC produce OCDO (Fig. S5). We have previously reported that DDA levels are decreased in human BC samples relative to normal tissues (3), whereas here we show that OCDO levels are increased in human BC samples compared with normal tissues. This indicates the existence of a metabolic balance between these two 5,6-EC derivatives in normal breast and BC that may either control or stimulate BC progression (Fig. S5). Interestingly, DDA inhibits the production of OCDO in BC cells through its action on ChEH, independently of ERα expression, and the inhibition of OCDO production contributes to the efficacy of DDA in vivo, indicating that the targeting of this oncometabolism could be relevant for BC treatment, and that treatment with DDA may compensate for its deficiency in BC. In addition, other ChEH inibitors, such as Tam or raloxifene (5), known to inhibit ERα and used as antiestrogen therapy in BC, block ChEH activity and OCDO production in ER^+ MCF7 and ER^- MDA-MB231 cells, indicating that these molecules target the OCDO pathway independently of ERα expression. We, and other laboratories, have previously reported that Tam inhibits the proliferation of MDA-MB231 cells and other ER^- BC cell lines (2, 32–34). These data suggest that the inhibition of the OCDO pathway may contribute to the antiproliferative effect of Tam in these ER^- BC cells, and thus that this molecule may be useful in the treatment of certain ER^- BC. This opens new avenues of research that deserve further study.

OCDO was previously described as a derivative of 5,6β-EC when it was found in the lungs of mice exposed to extreme conditions of oxidation, such as ozone exposure, but not under normal conditions (35). Consistent with our data, Pulfer et al. postulated the existence of an enzymatic mechanism to produce OCDO, since its formation requires living cells (35). 5,6-ECs were reported to be produced from cholesterol either by an enzyme not yet identified or via the autoxidation and lipoperoxidation of cholesterol to yield a mixture of 5,6-ECs, but with predominantly 5,6β-EC (1, 2). Since OCDO is a derivative of these compounds, conditions that generate oxidative stress and lipid peroxidation, such as chronic inflammatory processes, may therefore lead to OCDO production and be detrimental to DDA biosynthesis. Taking into account the fact that OCDO binds to the GR, its impact on inflammation deserves further study.

In the present study, IHC analyses indicated that the expression of all of the enzymes involved in the pathway producing OCDO, namely 11HSD2, D8D7I (EBP), and DHCR7, is higher in BC compared with NAT, while the enzymes that convert OCDO into CT (11HSD1 and H6PD) are weakly expressed in BC and NAT. Thus, the expression of these enzymes is consistent with both a higher production of OCDO in BC relative to NAT and with OCDO having tumor promoting properties. Accordingly, the analysis of several human BC mRNA databases also indicated that a high 11HSD2 expression or a low 11HSD1 expression correlates with a bad prognosis in BC patients. In addition, the elevated expression of DHCR7 and/or D8D7I (EBP) was associated with a bad survival outcome, and the risk of death was the highest when the expression levels of 11HSD2, DHCR7, and D8D7I (EBP) were taken into account, highlighting that the biosynthetic pathway producing OCDO is of major importance to BC pathology. Moreover, different studies revealed that high GR expression or activation correlated with poor therapeutic response or prognosis in $ERα^-$ breast cancers, as well as in many other solid tumors (36–40). Glucocorticoids exert complex and opposite effects and can enhance chemotherapy sensitivity by inhibiting cell proliferation or chemotherapeutic resistance by inducing cell survival and resistance to apoptosis (28). Interestingly, treatment with the GR antagonist, mifepristone (RU486), potentiates the antitumor efficacy of chemotherapy in ER^- BC mouse models (38). In $ERα^+$ breast cancer, GR expression has been associated with good clinical outcomes (37). The fact that glucocorticoids antagonize E_2-induced gene expression in BC cells (41) and up-regulate the enzyme involves in estrogen inactivation, may explain the better outcome in ER^+ BC patients expressing a high level of GR (42). Recently, liganded-GR was shown to repress a large ERα-activated transcriptional program by binding *in trans* to ERα-occupied enhancers. This event was associated with poorer metastasis-free outcomes in BC patients (43). These data highlight the important role of GR in BC and other tumors.

In conclusion, the discovery of OCDO, its proliferative effects through the GR, and the identification of the enzymes inducing or regulating its production are important findings, which should have major implications in the biology and diagnosis of BC and in the development of new therapeutic approaches. The targeting of the enzymes involved in cholesterol epoxide and glucocorticoid metabolism, as well as of the receptor mediating the proliferative effects of OCDO, represent new opportunities for therapeutic intervention in different BC subtypes, particularly in case of resistance to conventional therapies.

Experimental Procedures

For materials, animals, patient samples, and other techniques, see *SI Experimental Procedures*. All animal procedures concerning the care and use of laboratory animals were conducted according to the ethical guidelines of the Claudius Regaud Institute and followed the general regulations governing animal experimentation. All human samples were collected with the approval of the Institutional Review Board of the Claudius Regaud Institute, Toulouse, France and Tumor Bank Committee of the Claudius Regaud Institute, Institut Universitaire du Cancer Toulouse, France. Normal breast tissue was obtained from six patients who underwent mammoplasty and written informed consent was obtained before inclusion into the study. Patients' clinical characteristics and tumor pathological features were obtained from their medical reports and followed the standard procedures adopted by the Claudius Regaud Institute.

Metabolism of Sterols in BC Cells. Cells were plated into six-well plates (1×10^5 cells per well) in the appropriate complete medium. One day after seeding, this medium was replaced with complete medium without Phenol red supplemented with dextran-coated charcoal-stripped FBS, and cells were treated with either 0.6 μM [^{14}C]5,6α-EC for 72 h, 0.6 μM [^{14}C]5,6β-EC for 72 h, 1 μM [^{14}C]CT for 8 h, 1 μM [^{14}C]OCDO for 72 h, 0.2 μM [^{3}H]-CRT for 8 h, or 0.2 μM [^{3}H]cortisone for 72 h. After incubation, cells were washed and scraped, and neutral lipids were extracted with a chloroform-methanol mixture as described in Segala et al. (2), and then separated by TLC using either ethyl acetate as the eluent for [^{14}C]CT and [^{14}C]OCDO (9) or chloroform-methanol [87:13 (vol/vol)] for [^{3}H]-CRT or [^{3}H]cortisone in a method adapted from ref. 44. The radioactive sterols were revealed by autoradiography. For quantification, silica zones at the expected R*f* values corresponding to authentic [^{14}C]- or [^{3}H]-labeled standards were scraped and radioactivity was measured using a β-counter, as previously described (5).

Structural Characterization of the Unknown 5,6-EC Metabolite. MCF-7 cells (8×10^5 cells per dish) were treated with 10 μM 5,6α-EC. After a 72 h treatment, cells were washed twice with 5 mL PBS, then scraped and resuspended in 5 mL PBS and pelleted by centrifugation (800 × *g*, 5 min, 4 °C). Cells were then prepared for oxysterol analyses as previously described (2). Oxysterols were separated by RP-HPLC isocratically [MeOH:H_2O] (95/5) at a flow rate of 0.7 mL/min. CT and OCDO had retention times of 10 and 17 min, respectively, as previously described (9). The 9- to 11- and 15- to 17-min RP-HPLC fractions were dried under vacuum and submitted to chemical ionization-MS (CI-MS) analysis using ammonia as a reagent gas on a Perkin-Elmer SCIEX API 100 spectrometer.

GC/MS Quantification of Oxysterols. Tissues, tumors and cell homogenates were extracted as previously described (3). In a separate experiment, 0.1 μCi [^{14}C]OCDO was added to determine the yield of OCDO extraction. The samples were then dried under argon, dissolved in 1 mL toluene and passed through a silica cartridge (ISOLUTE SI 100 mg SPE Columns; Biotage). Oxysterol levels were determined by high-performance GC/MS detection using deuterium-labeled internal standards exactly as described in Iuliano et al. (45). The percentage of recovery of [^{14}C]OCDO was 96 ± 8%. The estimation of OCDO concentration in tumor xenografts or in patient tissues was calculated by assuming that 1 g of tissue corresponds to a volume of 1 mL (3).

ACKNOWLEDGMENTS. We thank R. M. Evans, H. Richard-Foy, V. Laudet, B. Staels, and M. Oulad-Abdelghani for the generous gifts of the indicated plasmids; Dr. N. Elarouci from the Carte d'Identité des Tumeurs (CIT) for performing the analyses according to tumor molecular subtype; and Dr. Stoney Simons Jr. (NIH) for critical reading of our manuscript. This work was funded by the Institut National de la Santé et de la Recherche Médicale, the Université de Toulouse; the Ministère Français de la Recherche et de l'Enseignement Supérieur through a predoctoral fellowship for 3 y (to M.V.); the fondation Association pour la Recherche sur le Cancer (ARC) Projet PJA 20131200342, plus the allocation of an ARC young researcher grant for 1 y (to M.V.); and International Neuroendocrine Cancer Alliance Translational Grant PRTK-K15-118 and the Initiatives d'Excellence (IDEX), Actions Thématiques Stratégiques (ATS) InnoVinBC, including a predoctoral fellowship for 3 y (to A. Mallinger).

1. Poirot M, Silvente-Poirot S (2013) Cholesterol-5,6-epoxides: Chemistry, biochemistry, metabolic fate and cancer. *Biochimie* 95:622–631.
2. Segala G, et al. (2013) 5,6-Epoxy-cholesterols contribute to the anticancer pharmacology of tamoxifen in breast cancer cells. *Biochem Pharmacol* 86:175–189.
3. de Medina P, et al. (2013) Dendrogenin A arises from cholesterol and histamine metabolism and shows cell differentiation and anti-tumour properties. *Nat Commun* 4:1840.
4. Silvente-Poirot S, Poirot M (2014) Cancer. Cholesterol and cancer, in the balance. *Science* 343:1445–1446.
5. de Medina P, Paillasse MR, Segala G, Poirot M, Silvente-Poirot S (2010) Identification and pharmacological characterization of cholesterol-5,6-epoxide hydrolase as a target for tamoxifen and AEBS ligands. *Proc Natl Acad Sci USA* 107:13520–13525.
6. Silvente-Poirot S, Poirot M (2012) Cholesterol metabolism and cancer: The good, the bad and the ugly. *Curr Opin Pharmacol* 12:673–676.
7. Leignadier J, Dalenc F, Poirot M, Silvente-Poirot S (June 19, 2017) Improving the efficacy of hormone therapy in breast cancer: The role of cholesterol metabolism in SERM-mediated autophagy, cell differentiation and death. *Biochem Pharmacol* 144c: 18–28.
8. Sevanian A, McLeod LL (1986) Catalytic properties and inhibition of hepatic cholesterol-epoxide hydrolase. *J Biol Chem* 261:54–59.
9. Voisin M, Silvente-Poirot S, Poirot M (2014) One step synthesis of 6-oxo-cholestan-3β,5α-diol. *Biochem Biophys Res Commun* 446:782–785.
10. Poirot M, et al. (2000) Synthesis, binding and structure-affinity studies of new ligands for the microsomal anti-estrogen binding site (AEBS). *Bioorg Med Chem* 8:2007–2016.
11. Lathe R, Kotelevtsev Y (2014) Steroid signaling: Ligand-binding promiscuity, molecular symmetry, and the need for gating. *Steroids* 82:14–22.
12. Chapman K, Holmes M, Seckl J (2013) 11β-hydroxysteroid dehydrogenases: Intracellular gate-keepers of tissue glucocorticoid action. *Physiol Rev* 93:1139–1206.
13. Odermatt A, Arnold P, Stauffer A, Frey BM, Frey FJ (1999) The N-terminal anchor sequences of 11beta-hydroxysteroid dehydrogenases determine their orientation in the endoplasmic reticulum membrane. *J Biol Chem* 274:28762–28770.
14. Atanasov AG, Nashev LG, Schweizer RA, Frick C, Odermatt A (2004) Hexose-6-phosphate dehydrogenase determines the reaction direction of 11beta-hydroxysteroid dehydrogenase type 1 as an oxoreductase. *FEBS Lett* 571:129–133.
15. Guedj M, et al. (2012) A refined molecular taxonomy of breast cancer. *Oncogene* 31: 1196–1206.
16. Madden SF, et al. (2013) BreastMark: An integrated approach to mining publicly available transcriptomic datasets relating to breast cancer outcome. *Breast Cancer Res* 15:R52.
17. Nelson ER, et al. (2013) 27-Hydroxycholesterol links hypercholesterolemia and breast cancer pathophysiology. *Science* 342:1094–1098.
18. Wu Q, et al. (2013) 27-Hydroxycholesterol promotes cell-autonomous, ER-positive breast cancer growth. *Cell Rep* 5:637–645.
19. Holbeck S, et al. (2010) Expression profiling of nuclear receptors in the NCI60 cancer cell panel reveals receptor-drug and receptor-gene interactions. *Mol Endocrinol* 24: 1287–1296.
20. Ratman D, et al. (2013) How glucocorticoid receptors modulate the activity of other transcription factors: A scope beyond tethering. *Mol Cell Endocrinol* 380:41–54.
21. Weikum ER, Knuesel MT, Ortlund EA, Yamamoto KR (2017) Glucocorticoid receptor control of transcription: Precision and plasticity via allostery. *Nat Rev Mol Cell Biol* 18: 159–174.
22. Kassel O, et al. (2001) Glucocorticoids inhibit MAP kinase via increased expression and decreased degradation of MKP-1. *EMBO J* 20:7108–7116.
23. Webster MK, Goya L, Ge Y, Maiyar AC, Firestone GL (1993) Characterization of sgk, a novel member of the serine/threonine protein kinase gene family which is transcriptionally induced by glucocorticoids and serum. *Mol Cell Biol* 13:2031–2040.
24. Jonat C, et al. (1990) Antitumor promotion and antiinflammation: Down-modulation of AP-1 (Fos/Jun) activity by glucocorticoid hormone. *Cell* 62:1189–1204.
25. Wang Y, et al. (2010) Modulation of retinoic acid receptor-related orphan receptor alpha and gamma activity by 7-oxygenated sterol ligands. *J Biol Chem* 285:5013–5025.
26. Soroosh P, et al. (2014) Oxysterols are agonist ligands of RORγt and drive Th17 cell differentiation. *Proc Natl Acad Sci USA* 111:12163–12168.
27. Deng R, Yang D, Yang J, Yan B (2006) Oxysterol 22(R)-hydroxycholesterol induces the expression of the bile salt export pump through nuclear receptor farsenoid X receptor but not liver X receptor. *J Pharmacol Exp Ther* 317:317–325.
28. Vilasco M, et al. (2011) Glucocorticoid receptor and breast cancer. *Breast Cancer Res Treat* 130:1–10.
29. Keenan CR, Lew MJ, Stewart AG (2016) Biased signalling from the glucocorticoid receptor: Renewed opportunity for tailoring glucocorticoid activity. *Biochem Pharmacol* 112:6–12.
30. Joshi T, Johnson M, Newton R, Giembycz M (2015) An analysis of glucocorticoid receptor-mediated gene expression in BEAS-2B human airway epithelial cells identifies distinct, ligand-directed, transcription profiles with implications for asthma therapeutics. *Br J Pharmacol* 172:1360–1378.
31. de Medina P, Paillasse MR, Payré B, Silvente-Poirot S, Poirot M (2009) Synthesis of new alkylaminooxysterols with potent cell differentiating activities: Identification of leads for the treatment of cancer and neurodegenerative diseases. *J Med Chem* 52: 7765–7777.
32. Gundimeda U, Chen ZH, Gopalakrishna R (1996) Tamoxifen modulates protein kinase C via oxidative stress in estrogen receptor-negative breast cancer cells. *J Biol Chem* 271:13504–13514.
33. Huang B, Warner M, Gustafsson JA (2015) Estrogen receptors in breast carcinogenesis and endocrine therapy. *Mol Cell Endocrinol* 418:240–244.
34. Payré B, et al. (2008) Microsomal antiestrogen-binding site ligands induce growth control and differentiation of human breast cancer cells through the modulation of cholesterol metabolism. *Mol Cancer Ther* 7:3707–3718.
35. Pulfer MK, Taube C, Gelfand E, Murphy RC (2005) Ozone exposure in vivo and formation of biologically active oxysterols in the lung. *J Pharmacol Exp Ther* 312: 256–264.
36. Chen Z, et al. (2015) Ligand-dependent genomic function of glucocorticoid receptor in triple-negative breast cancer. *Nat Commun* 6:8323.
37. Pan D, Kocherginsky M, Conzen SD (2011) Activation of the glucocorticoid receptor is associated with poor prognosis in estrogen receptor-negative breast cancer. *Cancer Res* 71:6360–6370.
38. Skor MN, et al. (2013) Glucocorticoid receptor antagonism as a novel therapy for triple-negative breast cancer. *Clin Cancer Res* 19:6163–6172.
39. Sorrentino G, et al. (2017) Glucocorticoid receptor signalling activates YAP in breast cancer. *Nat Commun* 8:14073.
40. Zhang C, et al. (2007) Clinical and mechanistic aspects of glucocorticoid-induced chemotherapy resistance in the majority of solid tumors. *Cancer Biol Ther* 6:278–287.
41. Karmakar S, Jin Y, Nagaich AK (2013) Interaction of glucocorticoid receptor (GR) with estrogen receptor (ER) α and activator protein 1 (AP1) in dexamethasone-mediated interference of ERα activity. *J Biol Chem* 288:24020–24034.
42. Gong H, et al. (2008) Glucocorticoids antagonize estrogens by glucocorticoid receptor-mediated activation of estrogen sulfotransferase. *Cancer Res* 68:7386–7393.
43. Yang F, et al. (2017) Glucocorticoid receptor:MegaTrans switching mediates the repression of an ERalpha-regulated transcriptional program. *Mol Cell* 66:321–331.e6.
44. Alikhani-Koupaei R, et al. (2007) Identification of polymorphisms in the human 11beta-hydroxysteroid dehydrogenase type 2 gene promoter: Functional characterization and relevance for salt sensitivity. *FASEB J* 21:3618–3628.
45. Iuliano L, et al. (2015) Cholesterol metabolites exported from human brain. *Steroids* 99:189–193.
46. Parks DJ, et al. (1999) Bile acids: Natural ligands for an orphan nuclear receptor. *Science* 284:1365–1368.
47. Wang Y, et al. (2010) Identification of SR1078, a synthetic agonist for the orphan nuclear receptors RORα and RORγ. *ACS Chem Biol* 5:1029–1034.
48. Cheng Y, Prusoff WH (1973) Relationship between the inhibition constant (K1) and the concentration of inhibitor which causes 50 per cent inhibition (I50) of an enzymatic reaction. *Biochem Pharmacol* 22:3099–3108.
49. Jézéquel P, et al. (2013) bc-GenExMiner 3.0: New mining module computes breast cancer gene expression correlation analyses. *Database (Oxford)* 2013:bas060.
50. Győrffy B, et al. (2010) An online survival analysis tool to rapidly assess the effect of 22,277 genes on breast cancer prognosis using microarray data of 1,809 patients. *Breast Cancer Res Treat* 123:725–731.